3214 J. Med. Chem. 2010, 53, 3214–3226
DOI: 10.1021/jm9018383

Journal of Medicinal Chemistry Article

Antimalarial versus Cytotoxic Properties of Dual Drugs Derived From 4-Aminoquinolines and Mannich Bases: Interaction with DNA

Nicole I. Wenzel,[†,+] Natascha Chavain,[‡,+] Yulin Wang,[§] Wolfgang Friebolin,[†] Louis Maes,[∥] Bruno Pradines,[⊥] Michael Lanzer,[§] Vanessa Yardley,[#] Reto Brun,[○] Christel Herold-Mende,[▽] Christophe Biot,[‡] Katalin Tóth,*[,◆] and Elisabeth Davioud-Charvet*[,†,¶]

[†]*Biochemie-Zentrum der Universität Heidelberg, Im Neuenheimer Feld 504, D-69120 Heidelberg, Germany,* [‡]*Université de Lille 1, Unité de Catalyse et de Chimie du Solide-UMR CNRS 8181, ENSCL, Bâtiment C7, USTL, B.P. 90108, F-59652 Villeneuve d'Ascq Cedex, France,* [§]*University of Heidelberg, Department of Infectiology, D-69120 Heidelberg, Germany,* [∥]*University of Antwerp, Groenenborgerlaan 171, B-2020 Antwerpen, Belgium,* [⊥]*Institut de Recherche Biomédicale des Armées antenne de Marseille, Unité de Recherche en Biologie et Epidémiologie Parasitaires, UMR 6236, Allée du Médecin-colonel Jamot, Le Pharo, BP 60109, F-13262 Marseille Cedex, France,* [#]*Department of Infectious and Tropical Diseases, London School of Hygiene & Tropical Medicine, Keppel Street, London WC1E 7HT, U.K.,* [▽]*Department of Neurosurgery, University of Heidelberg, D-69120 Heidelberg, Germany,* [○]*Swiss Tropical and Public Health Institute, Medical Parasitology and Infection Biology, CH-4002 Basel, Switzerland and University of Basel, Basel, Switzerland,* [◆]*Division Biophysics of Macromolecules, German Cancer Research Center, Im Neuenheimer Feld 580, D-69120 Heidelberg, Germany, and* [¶]*European School of Chemistry, Polymers and Materials (ECPM), Université de Strasbourg, 25 rue Becquerel, F-67087 Strasbourg Cedex 2, France.* [+] *These authors contributed equally to this work.*

Received December 13, 2009

The synthesis and biological evaluation of new organic and organometallic dual drugs designed as potential antimalarial agents are reported. A series of 4-aminoquinoline-based Mannich bases with variations in the aliphatic amino side chain were prepared via a three-steps synthesis. These compounds were also tested against chloroquine-susceptible and chloroquine-resistant strains of *Plasmodium falciparum* and assayed for their ability to inhibit the formation of β-hematin in vitro using a colorimetric β-hematin inhibition assay. Several compounds showed a marked antimalarial activity, with IC_{50} and IC_{90} values in the low nM range but also a high cytotoxicity against mammalian cells, in particular a highly drug-resistant glioblastoma cell line. The newly designed compounds revealed high DNA binding properties, especially for the GC-rich domains. Altogether, these dual drugs seem to be more appropriate to be developed as antiproliferative agents against mammalian cancer cells than *Plasmodium* parasites.

Introduction

Malaria remains one of the most prevalent diseases in the developing world. The most severe malaria episodes including cerebral malaria are due to *Plasmodium falciparum*. The rapid spread of multidrug resistance, especially toward chloroquine (CQ[a]), the main drug in use for many years, is a cause for major concern. The antimalarial agent amodiaquine (AQ) is effective against both CQ-susceptible and -resistant strains of *Plasmodium falciparum*. However, the development and clinical use of antimalarial 4-aminoquinoline agents such as AQ is limited in long-term treatments due to the cause of adverse side effects including hepatotoxicity and agranulocytosis when the drug is used for prophylaxis.[1] The mode of action of the 4-aminoquinoline antimalarial agents, which involves the inhibition of heme biomineralization,[2] is partly dependent on drug accumulation due to the lysosomotropism of these weak bases and a pH gradient between the cytosol and the acidic food vacuole of the parasite where host hemoglobin digestion occurs.[3]

Inside the red blood cells of the host, the malaria parasite degrades the hemoglobin for the acquisition of amino acids, i.e., to construct its own proteins, essential for energy metabolism and for parasitic growth and division. Digestion is carried out in an acidic compartment (pH ca. 5), the digestive vacuole, in the parasite. During this process, the parasite produces the toxic and soluble molecule heme and biocrystallizes it within or at the surface of lipids[4,5] to form hemozoin as the major detoxification product. CQ binds to heme (or ferriprotoporphyrin IX(Fe^{III}), FPIX) to form a FPIX−CQ complex which is highly toxic to the parasite and disrupts membrane function. Action of the toxic FPIX−CQ and FPIX ultimately results in parasite cell autodigestion. In essence, the parasite drowns in its own metabolic products.[6] Unfortunately the design and

*To whom correspondence should be addressed For E.D-C.: phone, +49-6221-54-4188; fax, +49-6221-54-5586; E-mail, elisabeth.davioud@gmx.de. For K.T.: phone, +49-6221-42-3390; fax, +49-6221-42-3391; E-mail, kt@dkfz.de.

[a] Abbreviations: AQ, amodiaquine; AT-rich DNA, DNA with high adenine (A)- and thymine (T)- base pair content; BCNU, 1,3-bis(2-chloroethyl)-1-nitroso urea; CQ, chloroquine; ΔT_m, difference between the melting temperature of the DNA treated with the drug and the temperature of the free DNA; FPIX, ferriprotoporphyrin IX; FQ, Ferroquine; GC-rich DNA, DNA with high guanine (G)- and cytosine (C)- base pair content; GSH, glutathione; HPLC, high pressure liquid chromatography; MDAQ, monodesethylamodiaquine; polydAdT, synthetic poly(dA-dT)-poly(dA-dT) double strand oligonucleotide; QN, quinine; t_R, retention time; RSH, thiol; T_m, the thermal dissociation temperature of DNA in the absence of any drug; $T_{m\ CQ}$, melting temperatures of DNA in the presence of CQ; $T_{m\ drug}$, melting temperatures of DNA in the presence of the drug; $T_m^{1/2}$, the middle of the peak at its half height; T_m^{int}, the middle of the integrated area below the derivative melting peak; T_m^{max}, the maxima of the derivative melting curves; TE buffer, 10 mM Tris-HCl 0.1 mM EDTA, at pH 7.4.

 Published on Web 03/23/2010

Scheme 1. Putative Bioactivation of Tertiary Amines by Oxidative *N*-Dealkylation Reactions (Pathway A) and Michael Addition Following Deamination of the Released Mannich Base (Pathway B)

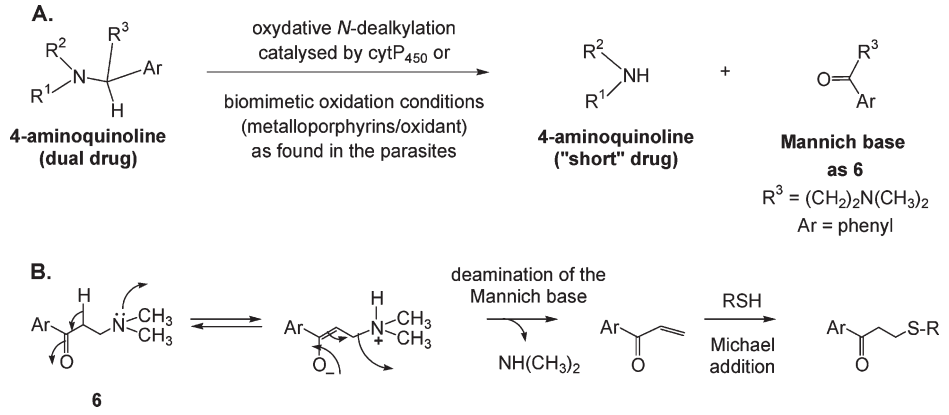

Chart 1. Structures of CQ, FQ, and Their Designed Related Analogues **1**−**5**

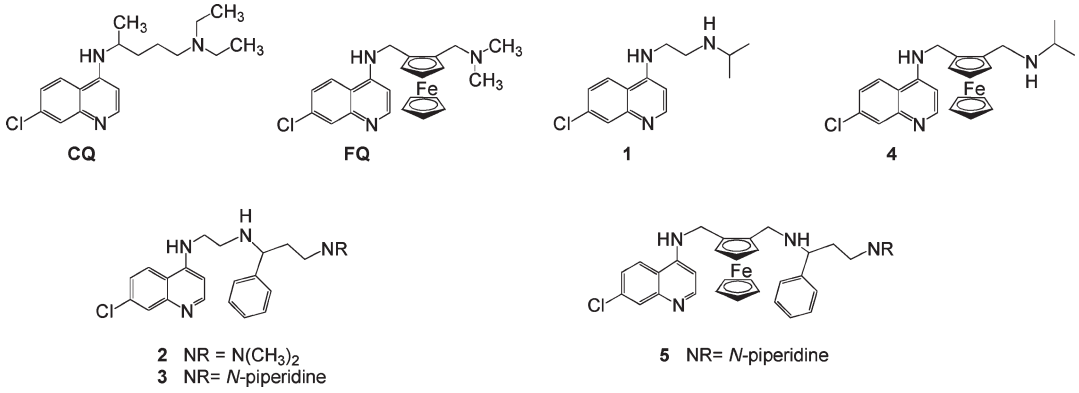

synthesis of new antimalarials are hindered by the fact that the mechanism of resistance is not fully understood and involves more than one altered function, e.g. related to drug transport,[7−10] redox equilibrium,[11] and metabolic pathways.[12]

As previously mentioned, the food vacuole of the malarial parasites is the locus of hemoglobin digestion leading to the release of an important amount of free heme. In the presence of reactive oxygen species, the released heme is thought to catalyze numerous oxidation reactions,[13] in particular with tertiary amine drugs (Scheme 1, pathway A). Recent advances aimed at understanding the drug catabolism were applied by using various iron porphyrins as models of cytP$_{450}$ enzymes to mimic the oxidative conditions found in the target cells.[14,15] Oxidative *N*-dealkylation of drugs is known to contribute both to biological activity and toxic effects of drugs.[16,17] Hence, drug bioactivation should be considered as a pro-drug strategy. On the basis of this hypothesis and on the knowledge of cytP$_{450}$ catalyzed oxidative *N*-dealkylation reactions,[18] we aimed at the design of new 4-aminoquinolines with an amino side-chain substituted by the aliphatic Mannich base according to a reductive amination. The dual drugs **2**, **3**, and **5** (Chart 1) are expected to enter the food vacuole of the parasite because of the recognized 4-aminoquinoline motif. The compounds **2**, **3**, and **5** were designed with the expectation that oxidative cleavage of such compounds in the food vacuole might generate two active compounds, a short CQ-analogue (active per se), and a thiol-reactive saturated Mannich base (Scheme 1, pathway B).

The modulation of the thiol attack, after the oxidative *N*-dealkylation, could be reached in this series of compounds by varying the pK_a value of amino group of the saturated Mannich base. The Michael acceptor properties of two saturated Mannich bases **6** and **7** (Chart 2) possessing a dimethylamine and a piperidine as amino leaving group were evaluated by the formation of the monoglutathionylated Mannich base adduct upon addition of one equivalent of glutathione. By increasing the stability of the drug, a higher amount of the nonoxidized compound (pro-drug) is expected to reach the parasite before oxidation in the host occurs.

Chart 2. Structures of the Mannich Bases **6** and **7** Used in the Study

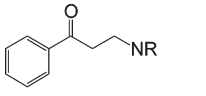

6 NR = N(CH$_3$)$_2$
7 NR = *N*-piperidine

Before evidencing the inhibition of β-hematin formation previous studies aimed at the understanding of the mode of action of CQ and other 4-aminoquinoline-based compounds demonstrated interactions of CQ with DNA in vitro.[19,20] But, as CQ is an inhibitor of lysosome maturation with high tropism for acidic compartments, relevance of correlation was debated.[21] The DNA:drug interaction has been studied by using different methods like spectrophotometry,[22] equilibrium dialysis[23] and viscosimetry,[24] fluorometry,[25] and DNA melting.[26,27] CQ, for example, strongly elevated the thermal dissociation temperature, T_m, of DNA. It was concluded that the drug forms a complex with DNA by ionic interaction

Scheme 2. Synthesis of the 4-Aminoquinoline Derivatives **2**−**3**, and **5**

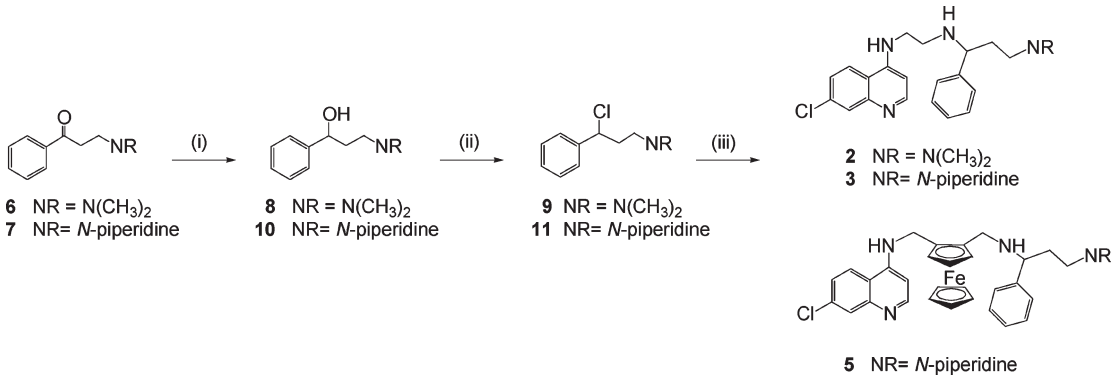

[a] Conditions: (i) NaOH, $NaBH_4$; (ii) $SOCl_2$, CH_3Cl, reflux; (iii) *N*-(7-Chloro-quinolin-4-yl)-ethane-1,2-diamine or *N*-[2-(aminomethyl)ferrocenyl]-7-chloroquinolin-4-amine, NEt_3, EtOH.

between the protonated ring system of CQ and the anionic phosphate groups of DNA and stabilizes the helical configuration against thermal denaturation[26,27] and a more specific interaction involving the aromatic cycles of CQ and the nucleotide bases. Later, it has been well documented that the buffering activity of CQ could improve transfection efficiency by facilitating DNA release from the endocytic pathway (as it may generate swelling and destabilization of endosomes) and/or by inhibiting lysosomal enzyme degradation. More recently, plasmid DNA, when bound by CQ, was shown to achieve improved gene transfer due to changes in its intracellular processing or its rate of intracellular degradation.[28] These data prompted us to evaluate the DNA binding capabilities of our new 4-aminoquinoline derivatives. Pollack et al. reported that the GC content of the DNA of *P. falciparum* is extremely low (17−19%), and the discrepancy between this result and previously reported values is due to the difference in purity of the free parasite preparations used for isolation of DNA.[29] However, CQ binds predominately to poly(dG-dC)·poly(dG-dC) than to other synthetic polynucleotides, and a conclusive link between DNA intercalation and the antimalarial activity of CQ has not been made so far.[30] At physiological and therapeutic conditions, a small number of binding sites could be occupied by CQ and the binding to these few sites could be enough to kill the parasite.[31] The unusually high AT content of the malaria parasite genome offers exceptional, yet unexploited, therapeutic opportunity.[32]

In this paper, we showed that the newly synthesized 4-aminoquinoline **1**−**5** derivatives interact with hematin in a fashion similar to CQ and FQ with respect to prevention of β-hematin formation in vitro. Furthermore, they displayed high antimalarial activity with IC_{50} and IC_{90} values in the low nM range but also a high cytotoxic potential against mammalian cells. On the basis of the knowledge that CQ and other 4-aminoquinoline-based compounds interact with DNA in vitro,[19] these data prompted us to evaluate the DNA binding capabilities of our new 4-aminoquinoline derivatives. Complex formation between DNA and drugs was first examined spectrophotometrically in order to gain information about the correlation between DNA binding and their cytotoxic properties. The possibility of the formation of complexes between certain drugs and DNA and thereby the ability to affect the biological properties and functions of DNA has been rather reliable demonstrated by other investigators.

Due to the fact that the human DNA exhibit a much higher GC content (43%) compared to *P. falciparum,* complexation studies involving our drugs with DNA preparations of two base ratios were further investigated to allow the comparison of the drug binding affinities specifically to GC- vs AT-rich regions and their cytotoxicity against mammalian cells. Taking into account the cytotoxicity of these dual drugs against mammalian cancer cells versus *Plasmodium* parasites implications for drug design will be discussed.

Results and Discussion

Chemistry. The synthetic route of the dual drugs described in Scheme 2 involves multiple steps starting from the saturated Mannich bases **6**−**7** obtained after a Mannich reaction with acetophenone, paraformaldehyde, and different amino hydrochlorides. Reduction of the keto group to the alcohols **8**,**10** with sodium borohydrate under basic conditions and the nucleophilic substitution of the hydroxyl group for a chloride upon thionyl chloride treatment led to compounds **9**,**10**. The second nucleophilic substitution of the chloride of **9**,**10** by *N*-(7-chloro-quinolin-4-yl)-ethane-1,2-diamine yielded to the favored 4-aminoquinoline-based compounds **2**−**3**. Compound **5** was prepared by nucleophilic substitution of **10** by *N*-[2-(aminomethyl)ferrocenyl)-7-chloroquinolin-4-amine. The nucleophilic substitution of **9** by *N*-[2-(aminomethyl)ferrocenyl)-7-chloroquinolin-4-amine failed whatever the conditions. The most difficult issue in the preparation of these compounds is the purification by flash chromatography. Only a small amount of product was obtained after two purification steps. Noteworthy is that the direct formation of the reductive amination products with the compounds **6**−**7** and *N*-(7-chloro-quinolin-4-yl)-ethane-1,2-diamine or *N*-[2-(aminomethyl)ferrocenyl)-7-chloroquinolin-4-amine under various conditions, e.g., $TiCl_4/NaBH_4$ or $NaBH(OAc)_3$,[33] and also the direct alkylation of the imine by β-aminoalkyllithium[34] failed, probably because of the deamination of the Mannich bases under these various conditions.

Glutathionylation of Mannich Base Derivatives. The Michael acceptor properties of the compounds **6** and **7** possessing one site for thiol alkylation were evaluated by the rate of formation of the monoglutathionylated Mannich base adducts upon addition of one equivalent of glutathione. The results were expressed as the time-dependent Mannich base:monoSG-adduct ratio given by HPLC retention times (HPLC t_R) and were shown in Figure S1 from the Supporting Information. The proposed mode of action toward thiols (RSH), like glutathione (GSH) by the saturated Mannich

Table 1. In Vitro Inhibition of β-Hematin Formation by 4-Aminoquinolines AQ, CQ, FQ, and Compounds **1**–**5** in MeOH/1N HCl (1:1)

compd	max inhibition reached (%) (at drug:hematin ratio)	IC_{50}
1	78 (3:1)	2.2
2	68 (3:1)	2.2
3	68 (3:1)	2.0
4[a]	90 (0.75:1)	0.2
5	63 (0.5:1)	0.4
AQ	100 (1.5:1)	0.6
CQ	73 (2:1)	1.5
FQ	72 (0.75:1)	0.3

[a] Data from ref 13.

bases **6** and **7** is shown in Scheme 1, pathway B. For the compounds **6** (t_R = 12.15 min) and **7** (t_R = 12.94 min), both generating the same glutathionyl-conjugate ($t_{R\ monoSG\text{-}adduct}$ = 13.11 min) after deamination, the Mannich base:monoSG-adduct ratio reached the value of 1 after 7.5 and 13 h, respectively. The replacement of the dimethylamine by a piperidine as leaving group of the saturated Mannich base derivatives gave a significant loss of reactivity. While the reactivity of Mannich bases to thiols was initially the basis to design antimalarial dual drugs described in this paper, we did not study further metabolism of the dual drugs under the biomimetic oxidative conditions expressed in the malarial parasites because of the very high toxicity of the compounds.

Inhibition Assay of β-Hematin Formation. Seven representative compounds, including CQ, the short CQ-analogue **1**, two aminoquinoline-based Mannich base derivatives **2** and **3**, and three ferrocenyl compounds, FQ, the FQ analogue **4**, and the ferrocenic dual drug **5**, were assayed for their ability to inhibit the formation of β-hematin in vitro using the colorimetric β-hematin inhibition screening assay with slight modifications described in the Experimental Section.[35] The results of the experiment were shown in Table 1, taking into account both the IC_{50} values and the drug:hematin ratio giving the percentage of maximal inhibition reached by the drug (reproducible data from two experiments). AQ was used as reference inhibitor of β-hematin formation because, with an IC_{50} value of 0.6 and 100% max inhibition at a drug:hematin ratio of 1.5:1, it presented the highest inhibitory capacity in the β-hematin formation assay, compared to CQ (IC_{50} of 1.5 and 73% max inhibition at a drug:hematin ratio of 2:1) and FQ (IC_{50} of 0.3 and 72% max inhibition at a drug:hematin ratio of 0.75:1) (Figure 1A). Under the conditions described above, the short CQ-analogue **1** and the Mannich base-derived 4-aminoquinoline dual drug **2** showed a similar inhibition behavior with an IC_{50} value of 2.2 but different maximal inhibition of 78% and 68%, respectively, at a drug:hematin ratio of 3:1 (Figure 1B). The nonferrocenyl dual drug analogue **3** and the ferrocenyl dual drug **5** displayed IC_{50} values of 2.0 and 0.4 with a maximal inhibition of 68% and 63% with a drug:hematin ratio of 3:1 and 0.5:1, respectively (Figure 1C). It is noteworthy that the inhibition behavior at high concentration of **5** is different compared to **3**, in a similar way between FQ and CQ (or AQ) observed in this study and previously discussed.[13] As observed for FQ itself (Figure 1A), an unusual bell-shaped curve giving the absorption at 405 nm versus drug:hematin ratio was also obtained for the FQ-analogue **5**, suggesting that apparent decreased inhibition of β-hematin formation at apparent high drug:hematin ratio might be due to an effective decreased drug:hematin ratio in the assay. Previous reports

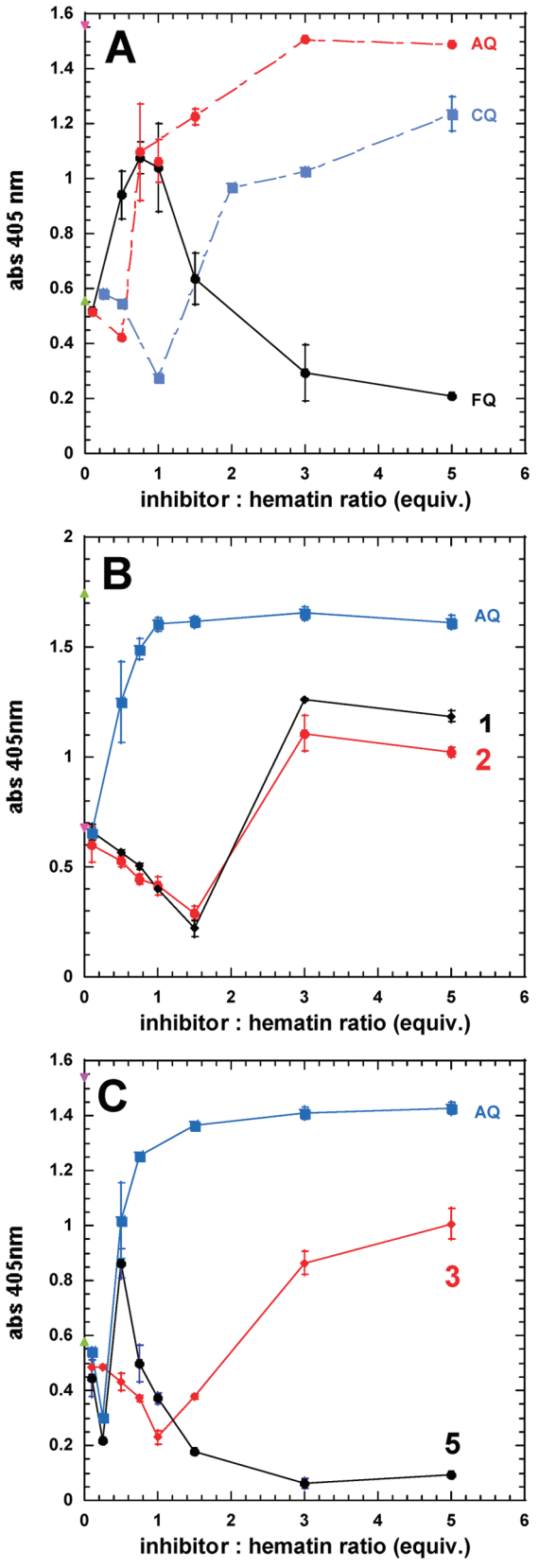

Figure 1. Inhibition of β-hematin formation. Absorbance measurements at 405 nm, performed in the β-hematin formation assay, in the presence of CQ, FQ, and compounds **1**–**5** with AQ as reference, were plotted as a function of the inhibitor:hematin ratio. The results are given in Table 1 as the IC_{50} values determined by the number of drug equivalents required to inhibit the β-hematin formation by 50%.

Table 2. Antimalarial Activities of the Short Analogues **1** and **4**, and the Dual Drugs **2**, **3**, and **5**, with Respect to CQ and FQ as References

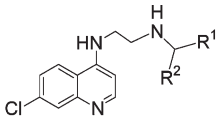

1 $R^1 = R^2 = CH_3$
2 R^1 = Ph, $R^2 = (CH_2)_2N(CH_3)_2$
3 R^1 = Ph, $R^2 = (CH_2)_2$piperidine

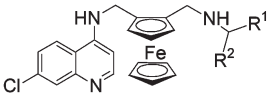

4 $R^1 = R^2 = CH_3$
5 R^1 = Ph, $R^2 = (CH_2)_2$piperidine

		IC_{50}			
compd	type	NF54[a] (nM)	K1[a] (nM)	Dd2[a] (nM)	MRC-5[b] (μM)
CQ	reference	11.2	316.3	527.0	64.0
1	CQ analogue	8.9	47.4	22.6	64.0
2	dual drug	7.1	61.9	25.6	27.0
3	dual drug	8.7	32.6	23.9	8.0
FQ	reference	11.9	20.0	1.6	6.0
4	FQ analogue	10.5	16.5	4.9	3.0
5	dual drug	12.7	15.9	5.2	1.0

[a] The standard drug chloroquine (CQ) and ferroquine (FQ) served as positive controls for the chloroquine-susceptible *Plasmodium falciparum* strain NF54 and two chloroquine-resistant *Plasmodium falciparum* strains K1 and Dd2. [b] The cytotoxicity is evaluated against this human lung cell line.

already discussed the importance of the ferrocenyl moiety in FQ in catalyzing the Fenton reaction under the specific oxidizing conditions found in the parasitic digestive vacuole.[36] While it has been well established that FQ, at high concentration, was able to self-aggregate in aqueous solution,[37] it rather seems that the appropriate redox behavior of FQ is responsible for destruction of the hematin:drug ratio by the Fenton reaction in the β-hematin assay.[13] The compound **5** might behave in the same way as FQ (Figure 1A,C).

Antiparasitic and Cytotoxic Activities. The antimalarial activities of the short CQ and FQ analogues, **1** and **4**, and the Mannich base-derived 4-aminoquinoline dual drugs **2**, **3**, and **5**, were first evaluated in a primary and secondary screenings against one CQ-susceptible and two CQ-resistant strains of *P. falciparum*, (Table 2). The cytotoxicity of the compounds was determined in assays using the human lung MRC-5 cell line (Table 2). Then, in a tertiary screening, the antimalarial potencies of the same compounds were confirmed against 12 strains of *P. falciparum* expressing a varying degree of resistance to established drugs, including CQ, quinine (QN), and monodesethylamodiaquine (MDAQ), the active metabolite of AQ. The data are presented as histograms in Figure 2A,B. They were derived from the IC_{50} and IC_{90} values given in the Supporting Information (Table S1). CQ, FQ, and MDAQ have been taken as internal references. All the short analogues and the 4-aminoquinoline-based Mannich base derivatives inhibited growth of *P. falciparum* strains in vitro whatever the susceptibility of the strain to CQ and MDAQ. The organic series is slightly more active than CQ or MDAQ on CQ- and MDAQ-susceptible strains, while the ferrocenic series showed a similar activity than CQ. On the other hand, the ferrocenic series presented a better activity on the CQ-resistant strains than the organic series, although this series showed a better activity than CQ (about 5 times more active). The dual drugs **2**, **3**, and **5** showed antimalarial activity in the same range as the corresponding short analogues **1** and **4** in the assays using NF54, K1, and Dd2 strains, but the effects were always more potent for the ferrocenic drugs **4** and **5** than for the nonferrocenic drugs **1**, **2**, and **3**. Using 12 strains of *P. falciparum*, the antimalarial activity of the compounds was represented as a function of the decreased susceptibility of the *P. falciparum* strain to CQ, QN, and MDAQ, expressed as IC_{50} (Figure 2A) and IC_{90} values (Figure 2B). We observed that the ferrocenic compounds like FQ maintained a constant antimalarial activity while the pure organic compounds, although remaining sharply more active than CQ, exhibited a slightly decreased activity on CQ- and MDAQ-resistant strains. These data suggested that a crossed resistance might be quickly at risk and developed for the organic series with respect to the established 4-aminoquinolines CQ, QN, and MDAQ. As showed previously, the presence of a ferrocenyl group seems to be a crucial character for a potent antimalarial activity on CQ-resistant strains.

The new 4-aminoquinolines showed a high antimalarial activity but also a high cytotoxicity on MRC-5 cell line (Table 2). The most cytotoxic molecules were the most active on CQ-resistant strains, i.e., ferrocenic compounds. In the organic series, the most cytotoxic compounds are the dual drugs and particularly **3** with a piperidine group. The cytotoxicity increased when the dimethylamino group is replaced by a piperidine group. Because the cytotoxicity of dual drugs was very important, we did not further design new optimized antimalarial dual drugs analogues, but instead we focused on a more comprehensive study on the factors responsible for the cytotoxicity.

In Vivo Antimalarial Activity against *Plasmodium berghei* in Mice. Two of the most antimalarial compounds **2** and **3**, in the organic series, were tested in *P. berghei*-infected ANKA mice by intraperitoneal administration. Conditions of in vivo screens for both compounds were conducted against CQ-susceptible *P. berghei*-infected mice according to the Peters's four-day test.[38] For comparative purposes, data acquired in the same screens for CQ and the two derivatives are included: CQ at 10 mg/kg po led to 99.2% reduction in parasitemia ($n = 5$ mice). Antimalarial activity of compound **2** against *P. berghei* ANKA in CD1 mice was evaluated at 30 mg/kg ip $\times$ 4. Four of the five animals died following the first drug injection, attesting for a very high toxicity of the compound in vivo. Furthermore, following ip administration of compound **3** in four animals (Swiss mice), all animals died due to serious toxic effects. While the dual drugs **2** and **3** showed high antimalarial activity, they also displayed very high toxicity. The observation made with CQ and other 4-aminoquinoline-based compounds interacting with DNA in vitro prompted us to study the antiproliferative activity and the binding of the newly designed dual drugs to DNA in order to understand the origin of their cytotoxic properties.

Proliferation Assays. Because of the cytotoxicity and the interaction of our compounds with DNA, we tested our 4-aminoquinolines for their anticancer activity. The short analogues and the dual drugs **1**−**5** were tested on the glioblastoma carmustine-resistant cell line NCH89 (carmustine namely BCNU) (Table 3). The obtained IC_{50} values on glioblastoma carmustine-resistant cells are in accordance with the cytotoxycity of the compounds. The most cytotoxic molecules against human MRC-5 cells displayed the most potent antiproliferative effect to kill the glioblastoma carmustine-resistant cells. Compared to CQ, FQ, and their short analogues, we observed a significant higher antiproliferative effect with the dual drugs (Figure 3). Also, the ferrocenic was always found more active than the organic

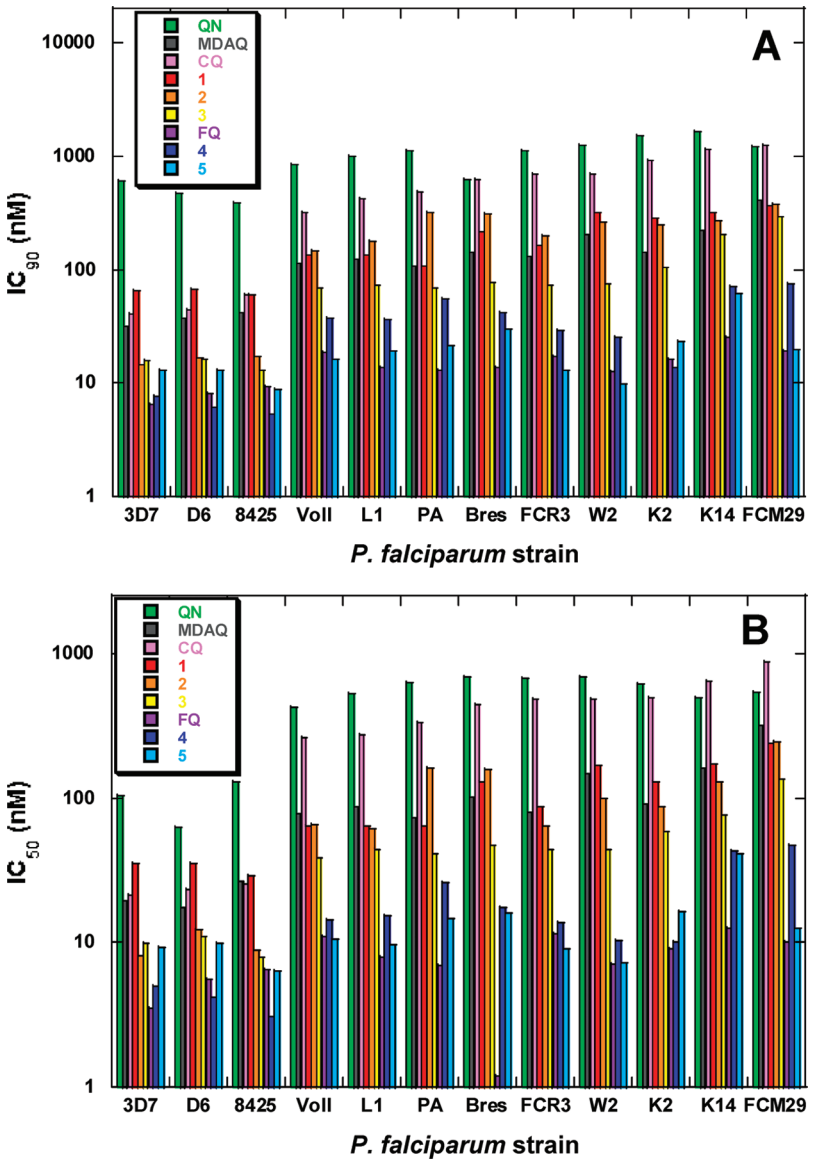

Figure 2. Antimalarial activities of 4-aminoquinolines **1**−**5** against various *P. falciparum* strains.

Table 3. Antiproliferative Effects of CQ, FQ, and Compounds **1**−**5** (IC_{50} Values) on the NCH89 Glioblastoma Cells

	compd						
NCH89[a] cell line	CQ	**1**	**2**	**3**	**FQ**	**4**	**5**
IC_{50} (μM)	41.2	30.4	7.3	5.6	4.0	3.4	1.5
SD (μM)	±7.4	±1.3	±0.4	±0.01	±0.1	±0.1	±0.008

[a] IC_{50} of carmustine = 615 ± 38 μM

series, both in terms of cytotoxicity and antiproliferative properties. By far, combination of the ferrocene moiety and the drug duality by linking a 4-aminoquinoline to the Mannich base through reductive amination increased both the cytotoxicity and the antiproliferative capability of final molecules (Figure 3). Recently, combination of Ru^{II} and chloroquine in the same molecular structure, stabilized by arene ligands, was shown to result in enhanced activities against resistant malaria parasites and against certain types of cancer cells.[39] Compared to the short CQ analogues, the presence of both an additional amino group in the side chain and an aryl group might significantly modify the partition coefficients of the dual drugs inside the parasite, in agreement with the calculated pK_a values of some representatives of the organic series (Table S2 in the Supporting Information). It is well-known that CQ increased the gene transfection and that the number, nature, and location of charges dramatically change the transfection properties of the cationic aminoside chain of CQ analogues.[28,40] Varying the charge per molecule might have a profound effect on the buffering power to promote endosomal escape from endocytic pathway and DNA binding and trafficking, processing, or degradation of DNA within the cells.

DNA Binding Studies. The spectrophotometric method used in the DNA interaction study allowed the determination of the complex formation between the drugs and the DNA evidenced by a change in the absorption spectra of the ligand upon addition and binding to DNA. The stepwise addition of small increments of DNA to a solution containing a constant concentration of the drug (e.g., 10 μM of **1**) at physiological pH is shown in Figure 4. An increase of absorption at 260 nm (characteristic for DNA), indicating the higher concentration of DNA is ascertained. A progressive

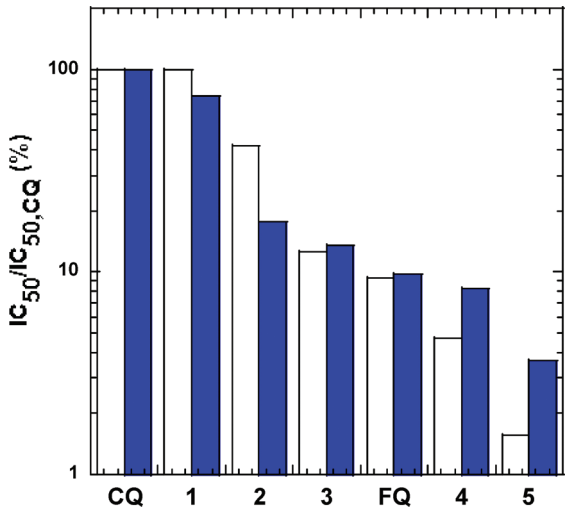

Figure 3. Cytotoxicity versus antiproliferative activity of FQ and compounds **1**−**5**, relatively to CQ. The ratios of IC_{50} values for studied drugs to the IC_{50} value for CQ in the assays performed (i) for the evaluation of the cytotoxicity against human MRC-5 (empty bars), (ii) for the evaluation of the antiproliferative effects against human glioblastoma carmustine-resistant cells (blue bars), were plotted (see IC_{50} values listed from Tables 2 and 3). Within each series, organic or ferrocenic, the dual drugs showed the most important toxicity relative to their parent representative, CQ or FQ.

decrease at 320 and 340 nm (characteristic for the quinoline ring) and a shift of around 10 nm toward longer wavelengths of the absorption peaks of the drugs is observed because more and more drug is bound to DNA. The decrease of the absorption is due to the intercalation of the quinoline into DNA and is higher than the decrease due to the dilution effect. Cohen et al. have already observed the same phenomenon for CQ in 1965 and has shown that the shift toward longer wavelengths is characteristic for the formation of a quinoline/DNA complex.[27] The appearance of an isosbestic point around 342 nm indicated that the limiting systems (i.e., the spectra of free and completely bound drug) intersect and allowed the selection of a single wavelength for the study of complex formation. This phenomenon was observed for all studied compounds. The initial absorbance spectra of the compounds are shown in Figure S2 in the Supporting Information. Molar extinction coefficients were determined in aqueous solutions, methanol and toluene, and shown in the Supporting Information (Tables S3 and S4).

A more sensitive evaluation of the interaction of the 4-aminoquinolines with DNA was achieved by using the spectrofluorometry. It enables noise-free quantitative measurements with one to two order lower concentrations of the drugs than through the absorption. The emission of the drugs was measured with the optimal excitation wavelength of 320 nm, separating sufficiently the fluorescence emission from the Raman scattering of water (360 nm) (Figure 5A,B). The organic compounds showed high emission due to the presence of the quinoline ring characterized by a large fluorescence band at around 380 nm, with high variability in fluorescence intensity and quantum yield (Figure 5A and Table S5 in the Supporting Information). Only the spectrum of CQ is 5 nm red-shifted. The high emission observed for **1** was found quenched in the case of both dual drugs **2**, **3** containing one phenyl group. Compared to compounds **1** and **4**, both substituted by a short amino side chain, CQ and FQ displayed a much lower emission signal. Addition of

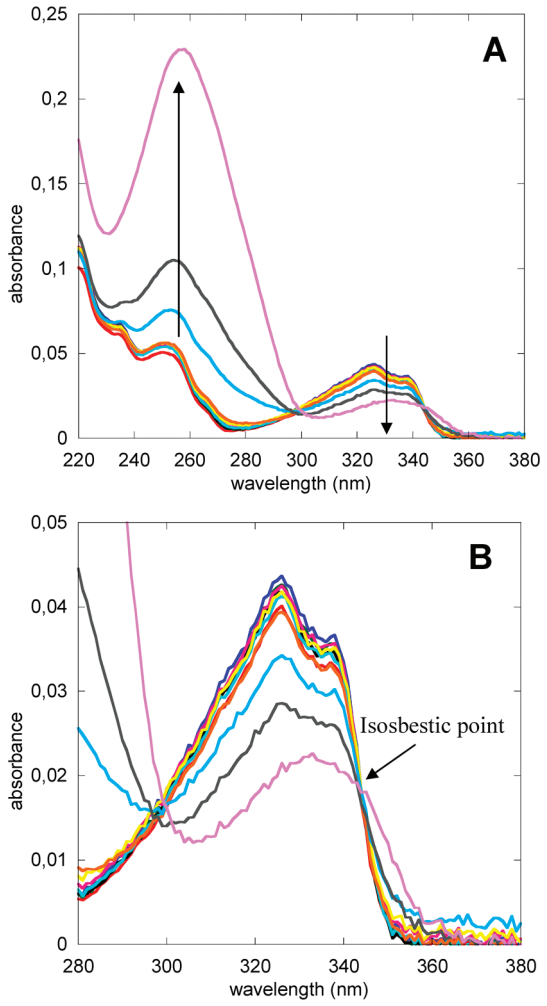

Figure 4. Absorption spectrum of a 10 μM inhibitor **1** solution upon addition of a DNA solution in increasing concentration. The binding to a linear double stranded DNA (containing 50% AT) was investigated by UV−Vis spectrometry (A). Increased absorption at 260 nm corresponds to the DNA concentration. DNA induces significant changes in the spectra with a marked decrease in absorption of the free 4-aminoquinoline ligand around 320 and 340 nm, while an increased absorption is observed for the DNA-ligand complex shifted to a longer wavelength around 350 nm ((B) zoom between 280 and 380 nm).

DNA induces a monotonous decrease of the fluorescence indicating the drug binding (data not shown). In contrast to the organic drugs, the ferrocenic compounds showed very low emission, around 10-fold less, and the emission signal was compromised by the Raman scattering (Figure 5B). The observed weak emission is probably due to a quenching of fluorescence because of the presence of the ferrocene group. In this way, the use of the spectrofluorometric method for the quantitative titration of the ferrocenic compounds was not possible.

A precise titration by addition of a DNA solution to a 1−10 μM drug solution was followed by spectrofluorometry for the organic compounds and by UV-spectrophotometry for all compounds (10 μM). To evaluate quantitatively the binding of the drugs with DNA, the dissociation constants were determined. In our case, due to the multiple binding modes, the Scatchard representation is not usable and the fit of the titration curves was too complex. However, we estimated the dissociation constants by taking the total

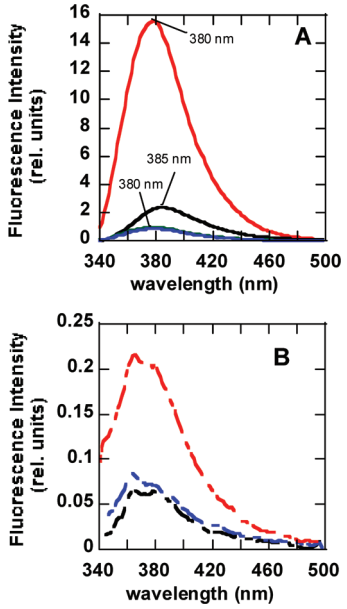

Figure 5. Fluorescence spectra of CQ, FQ, and 4-aminoquinolines **1**−**5** measured in aqueous solution. The fluorescence emission spectra for organic (A) and ferrocenic (B) compounds were illustrated as CQ, (black full); FQ, (black, dashed); 1, (red, full); 4, (red, dashed); 2, (green, full); 3, (blue, full); 5, (blue dashed). Measurements were performed in TE buffer containing 5 mM NaCl, with excitation at 320 nm, spectra are corrected for the buffer signal and instrument response.

Table 4. K_d Values of CQ, FQ, and Compounds **1**−**5** Estimated by UV−Vis Spectrophotometry and Spectrofluorometry at Low Ionic Force (μ = 12 mM)

	K_d, μM	
compd	by absorption	by emission
CQ	7.5	9.0
1	17.5	8.0
2	7.0	8.0
3	1.0	4.0
FQ	5.0	
4	8.0	
5	0.2	

DNA concentration added in the curve when half of the drug is bound to DNA. The dissociation constants were estimated at a low ionic force of 12 mM at pH 7.5. The dissociation constants indicated that all our drugs showed a high affinity for DNA (Table 4). For CQ, the determined K_d value was in the same order, as reported by Viola et al. in a similar experiment.[41] The dual drugs **3** and **5** containing the piperidine group displayed a better affinity toward the DNA with K_d values of 1.0 and 0.2 μM, respectively. These results are in accordance with the highest cytotoxicity and the most potent antiproliferative effect of these two compounds in each series, i.e., in the organic and the ferrocenic series.

The interaction between the drugs and DNA could also be sensitively recognized due to the stability changes in macromolecules. The cooperativity of the thermal denaturation amplifies the effect of the local interactions: one from thousand base pairs involved in an interaction may be detectable. The effect of the drugs on thermal stability of DNA indicating possible structural changes was measured by UV absorption melting. Intercalation of molecules into the double helix is known to stabilize the DNA against

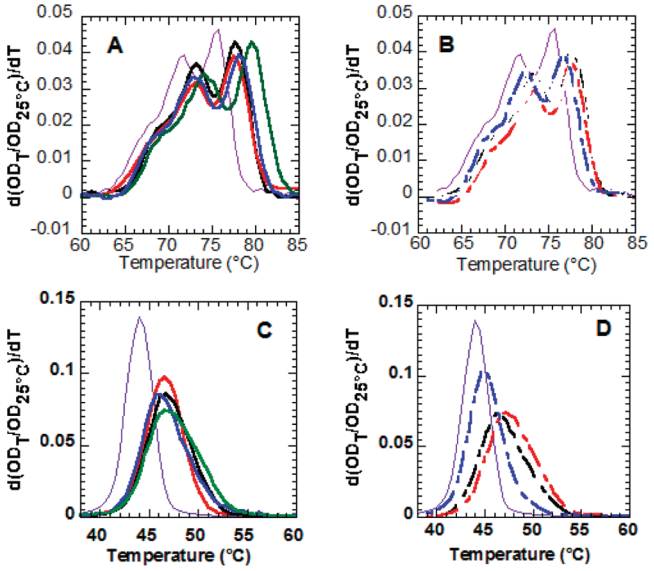

Figure 6. Derivative melting curves of two different DNAs in the presence of CQ, FQ, and 4-aminoquinolines **1**−**5**. The derivative melting curves of 50% (A,B) and 100% AT rich (C,D) DNA treated with organic (A,C) and ferrocenic (B,D) compounds were illustrated as in Figure 4, while DNA alone is shown with mauve full line. The thermal denaturation was measured in TE buffer containing 5 mM NaCl, at base pair:drug molar ratio of 15:1.

thermal strand separation and thus to increase T_m.[26] The effect of the drugs on the derivative melting curves of two DNA types is presented in Figure 5. To study also the role of DNA base composition in the drug binding, we compared a DNA with 50% AT content: a linearized pUC18 plasmid (Figure 6A,B) to a synthetic polydAdT double-strand oligonucleotide (Figure 6C,D). This oligonucleotide has been chosen because of the unique AT-richness of *Plasmodium* genome (80% AT, relative to 60% in human DNA), especially in the intergenic regions (more than 90%).[42]

For all compounds, the thermal stability of both DNA increased, evidencing the interaction of the drugs with DNA in a slightly varying extent. The stabilization was proportional to the drug concentration and depended on the base pair/drug molar ratio (data not shown). The data presented in Figure 5 showed the results obtained at 1 μM drug concentration in a 15 base pair:drug ratio. All characteristic melting temperatures are listed in Table S5 of the Supporting Information. As an observed feature, the ferrocenic dual drug **5** has significantly smaller effect on both DNAs than any other compound. This is in apparent contrast with the very low dissociation constant evaluated for this compound (Table 4). One possible cause might be linked to the Fenton catalyst properties of these ferrocenic 4-aminoquinolines,[36] in agreement with the destruction of the drug:hematin ratio observed in the β-hematin inhibition assay. The dual drug with a terminal *N*,*N*-dimethyl amine **2** is the most stabilizing ligand of 50% AT-containing DNA, while the short FQ analogue **4** is the most stabilizing agent of polydAdT. The difference between the melting temperature of the DNA treated with the drug and the temperature of the free DNA (ΔT_m) gives quantitative information about the force of the interaction between the drug and the DNA. On the other side, this difference is also dependent on the free DNA alone. To avoid this effect, we compared the DNA stabilization by one compound with the stabilization caused

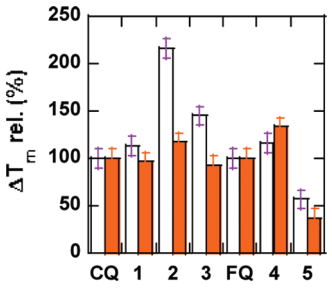

Figure 7. Illustration of the different stabilizing effects of FQ and 4-aminoquinolines **1**−**5** relative to CQ. ΔT_m rel is the change in melting temperature $T_m{}^{int}$ of a drug relative to the change produced by CQ, expressed in %. Empty bars were plotted for 50% AT-containing DNA and red bars for 100% AT-rich DNA. $T_m{}^{int}$ values were taken from Figure 5 and listed in Table S5.

by CQ on the same DNA type. The relative ΔT_m (ΔT_m rel) was defined in the following equation:

$$\Delta T_m \text{ rel } (\%) = (T_{m\,drug} - T_m) : (T_{m\,CQ} - T_m)$$

where $T_{m\,drug}$, $T_{m\,CQ}$, and T_m are the melting temperatures of DNA in the presence of the drug, or of CQ, or in the absence of any drug, respectively. For this calculation, we took the $T_m{}^{int}$ values obtained as the middle of the integrated area below the derivative melting peaks, which is the most insensitive parameter to the type of DNA. The ΔT_m rel values relative to CQ (Table S5, Supporting Information) were plotted in Figure 7. Only the dual drugs **2**, **3**, and **5** showed a significantly higher affinity toward the GC- vs the AT-rich regions. Interestingly, the same dual drugs showed the highest antiproliferative effects compared to the activity of short analogues (Table 3).

Conclusion

Our original reason for embarking on an investigation of the interaction of 4-aminoquinoline derivatives with two different types of DNA was for the purpose of understanding the high cytotoxicity of our designed antimalarial dual drugs. Research of DNA binding is important for the design of novel antimalarial agents to prevent the interaction of drug into host DNA and to decrease their human cytotoxicity. Noteworthy is the fact that DNA binding studies have to be taken with caution toward the relevance of the mechanism of drug action in vivo because the pharmacokinetics of the drug in the cells do not necessarily reflect the observations made in experiments in vitro with isolated targets. For more than 60 years, the DNA binding properties of CQ have not compromised the success of the use of CQ as antimalarial drug in human medicine. More work need to be continued to know if FQ, which is in clinical trials, will be a successful antimalarial drug as much as CQ was. However, the structural changes in the side chain of CQ might dramatically affect the endosomal escape, the DNA binding and trafficking, processing, or degradation of DNA within the cells, as observed in gene expression and transgene expression by CQ analogues.[28] Altogether our dual drugs seem to be more appropriate to be developed as antiproliferative derivatives against mammalian cancer cells than *Plasmodium* parasites. Furthermore, our findings based on the observed interaction of newly designed 4-aminoquinolines with GC-rich DNA revealed the possibility to specifically target the GC-rich domains of DNA. Future directions are aimed at the evaluation of gene transfection and delivery through endosomal escape properties of organic dual drugs through the buffering capabilities of their polyamine side chain.

Experimental Section

Chemistry. Melting points were determined on a Büchi melting point apparatus and were not corrected. ^{1}H (300 MHz) and ^{13}C (75 MHz) NMR spectra were recorded on a Bruker DRX-300 spectrometer and a Bruker AC 300 spectrometer; chemical shifts were expressed in ppm relative to TMS; the protons are indicated as QnH (H linked to 4-aminoquinoline), H-Pip (H linked to the piperidine moiety), and PhH (H linked to phenyl); in the ^{1}H spectra multiplicity is indicated as s (singlet), d (doublet), t (triplet), and m (multiplet); C indicates a quaternary carbon in ^{13}C spectra. Elemental analyses were carried out at the Mikroanalytisches Laboratorium der Chemischen Fakultät der Universität Heidelberg. MALDI-TOF and ESI-MS were recorded at facilities of the Institut für Organische Chemie der Universität Heidelberg and at the Centre Commun de Mesures de l'Université des Sciences et Technologies de Lille, respectively. Analytical TLC was carried out on precoated Sil G-25 UV_{254} plates from Macherey-Nagel, detection by UV lamp. Flash chromatography was performed using silica gel G60 (230−400 mesh) from Macherey-Nagel. The unsaturated Mannich base 1-(2-chlorophenyl)-5-(dimethylamino)-pent-1-en-3-one hydrochloride, the CQ-analogue *N*-(7-Chloro-quinolin-4-yl)-*N*′-isopropyl-ethane-1,2-diamine **1**, and *N*-(7-Chloro-quinolin-4-yl)-ethane-1,2-diamine were synthesized as previously described.[43,44] The saturated Mannich base **7** (mp 192−193 °C) was prepared via a nucleophilic substitution reaction of *p*-chloropropiophenone, piperidine, and $CsCO_3$. 3-Dimethylamino-1-phenyl-1-propanol **8** was prepared by $NaBH_4$ reduction of the commercially available *N*,*N*-dimethylaminopropiophenone hydrochloride **6** according to reported procedures.[45] 1-Phenyl-3-piperidin-1-yl-propan-1-one **7** was reduced with an excess of sodium borohydride in methanol at 0 °C to the 1-phenyl-3-piperidin-1-yl-propan-1-ol **10**. 3-Chloro-*N*,*N*-dimethyl-3-phenylpropan-1-amine hydrochloride **9** and 1-(3-chloro-3-phenylpropyl)piperidine hydrochloride **11** were prepared from the corresponding alcohols, 3-(dimethylamino)-1-phenylpropan-1-ol **8**, and 1-phenyl-3-(piperidin-1-yl)propan-1-ol **10**, by action of thionyl chloride in chloroform under heating to reflux as previously reported.[46] 7-Chloro-quinolin-4-yl-[3-(isopropylaminomethyl)-ferrocenyl]-amine **4** was synthesized as previously described.[13] The purity of compounds **2**, **3**, and **5** was controlled by melting points, and elemental analyses that agreed with the calculated values within 0.4%. Analytical high pressure liquid chromatography (HPLC) was performed on a Spectra system equipped with a UV detector set at 254 nm and using two types of high pressure liquid chromatography (HPLC) columns, a Macherey-Nagel C18 Nucleosil column (4 mm × 300 mm, 5 μm, 100 Å) or Macherey-Nagel EC 250/4.6 Nucleodur 100−5 CN-RP (4 mm × 300 mm, 5 μm, 100 Å). Compounds were dissolved in acetonitrile and injected through a 50 μL loop. The following solvent systems were used: eluent (A): 0,05% trifluoroacetic acid (TFA) in H_2O, eluent (B) 100% CH_3CN. HPLC retention times (HPLC t_R) were obtained, at flow rates of 1 mL/min, using the following conditions: 100% eluent A for 5 min, then a gradient run to 100% eluent B over the next 20 min.

***N*^{1}-[2-(7-Chloro-quinolin-4-ylamino)-ethyl]-*N*^{3},*N*^{3}-dimethyl-1-phenyl-propane-1,3-diamine (2 Base and 2 Chlorhydrate Salt).** 7-Chloro-(quinolin-4-yl)ethane-1,2-diamine (400 mg, 1.80 mmol) was dissolved in anhydrous ethanol (35 mL) under heating. After cooling to room temperature, triethylamine (1.26 mL, 9.02 mmol) was added. Then the 3-chloro-*N*,*N*-dimethyl-3-phenylpropylamine hydrochloride was added as solid in three portions: first, 444 mg (1.89 mmol), then further 92 mg (0.39 mmol) after 18 h and then 51 mg (0.22 mmol) after further 7 h. After additional 15 h stirring at room temperature, the solvent was evaporated and the residue was purified by flash chromatography

(first on neutral Al_2O_3 with $CHCl_3/CH_3OH$ 40:1 and then, on SiO_2 with acetone/methanol/water/triethylamine 10:3:2:0.2) to yield the base **2** as a colorless oil/solid (0.43 g, 1.12 mmol, 62%); mp (°C): 210−212. ^{1}H NMR (300 MHz, $CDCl_3$) δ (ppm): 8.37 (d, 1H, ^3J = 6 Hz, QnH-2), 7.86 (d, 1H, J = 2 Hz, QnH-8), 7.74 (d, 1H, J = 9 Hz, QnH-5), 7.25 (m_c, 5H, PhH), 7.18 (dd, 1H, J = 2 Hz, J = 9 Hz, QnH-6), 6.26 (s_{br}, 1H, NH), 6.18 (d, 1H, ^3J = 6 Hz, QnH-3), 4.37 (s_{br}, 1H, NH), 3.66 (t, 1H, ^3J = 6 Hz, CH), 3.19 (m, 2H, NCH_2), 2.84 (m, 1H, NCH_2), 2.73 (m, 1H, NCH_2), 2.33 (m, 1H, NCH_2), 2.21 (m, 1H, NCH_2), 2.12 (s, 6H, CH_3), 1.92 (m, 1H, CH_2NMe_2), 1.77 (m, 1H, CH_2NMe_2). ^{13}C NMR (75 MHz, $CDCl_3$) δ (ppm): 151.5 (CH), 149.9 (C), 148.6 (C), 142.9 (C), 134.6 (C), 128.5 (CH), 128.0 (CH), 127.3 (CH), 126.9 (CH), 124.9 (CH), 121.7 (CH), 117.2, 98.7 (CH), 61.9 (CH), 57.0 (CH_2), 45.2 (CH_3), 44.8 (CH_2), 41.9 (CH_2), 35.0 (CH_2). The chlorhydrate salt of **2** was prepared by solubilizing the compound in a minimum of methanol (2 mL) and 4 equiv of TMSCl was added. The precipitated hydrochloride was separated by filtration, crystallized in ethanol, washed with cold ether, and dried. MS (FAB^+-MS) m/z: 383.4 (MH+). Anal. $C_{22}H_{30}N_4.3HCl\cdot0.35H_2O$.

***N*-[(7-Chloro-quinolin-4-yl)-ethyl]-*N'*-(1-hexazin-1-yl-3-piperidin-1-yl-propyl)-ethane-1,2-diamine hydrochloride 3.** *N'*-(7-Chloroquinolin-4-yl)-ethane-1,2-diamine (400 mg, 1.80 mmol) was dissolved in anhydrous ethanol under heating. After cooling to room temperature, an excess of triethylamine (1.26 mL, 9.02 mmol) was added. Then 1-(3-chloro-3-phenylpropyl)piperidine hydrochloride (693 mg, 2.53 mmol) was added as solid in three portions during 2 days. After additional stirring at room temperature, the solvent was evaporated in vacuo and the residue was purified by flash-chromatography on neutral Al_2O_3 ($CHCl_3$/CH_3OH 40:1) to obtain the base **3** as a colorless solid (140 mg; 0.33 mmol, 18%). The chlorhydrate salt of **3** was prepared as previously described for **2**; mp (°C): 121−125. ^{1}H NMR (300 MHz, $CDCl_3$) δ (ppm): 8.26 (d, 1H, J = 5.31 Hz, QnH-2), 7.73 (s, 1H, QnH-8), 7.59 (d, 1H, J = 8.94 Hz, QnH-5), 7.16−7.04 (m, 6H, PhH + QnH-6), 6.07 (d, 1H, J = Hz, QnH-3), 5.91 (s_{br}, 1H, NH), 3.52 (t, 1H, J = 5.35 Hz, CH), 3.13−2.85 (m, 2H, NCH_2), 2.79−2.50 (m, 2H, NCH_2), 2.31−1.90 (m, 5H, CH_2 + H-Pip), 1.90−1.45 (m, 2H, CH_2), 1.45−1.05 (m, 7H, H-Pip). ^{13}C NMR (75 MHz, $CDCl_3$) δ (ppm): 151.67 (CH), 149.82 (C), 148.81 (C), 143.42 (C), 134.47 (C), 128.34 (CH), 128.20 (CH), 127.07 (CH), 126.81 (CH), 124.80 (CH), 121.61 (CH), 117.22 (C), 98.81 (CH), 62.32 (CH), 56.65 (CH_2), 54.37 (CH_2), 44.96 (CH_2), 42.17 (CH_2), 34.36 (CH_2), 25.57 (CH_2), 23.96 (CH_2). MS (MALDI-TOF) m/z: 423.5 (M+). Anal. $C_{25}H_{31}ClN_4\cdot2.8HCl\cdot1.9H_2O$.

7-Chloro-*N*-(2-{[1-phenyl-3-(piperidin-1-yl)propylamino]methyl}-ferrocenyl)quinolin-4-amine 5. *N*-[2-(Aminomethyl)ferrocenyl)-7-chloroquinolin-4-amine (234 mg, 0.58 mmol) was dissolved in anhydrous ethanol. After complete dissolution, an excess of triethylamine (5 equiv) and 1-(3-chloro-3-phenylpropyl)piperidine hydrochloride (134 mg, 0.52 mmol) were added. The mixture was stirred for 5 h at room temperature. After the addition of 1-(3-chloro-3-phenylpropyl)piperidine hydrochloride (28 mg, 0.11 mmol), the reaction mixture was allowed to stir for further 3.30 h. Then the solvent was evaporated in vacuo and the residue was purified by flash-chromatography on silica gel ($EtOAc/NEt_3$ 97.5:2.5) to obtain the base **5** as a brown solid (28 mg; 0.04 mmol, 6%); mp (°C): 59−62. ^{1}H NMR (300 MHz, $CDCl_3$) δ (ppm): 8.49 (d, 1H, J = 3.9 Hz, QnH-2), 7.87 (d, 1H, J = 4.2 Hz, QnH-8), 7.79 (d, 0.5H, J = 9.0 Hz, QnH-5), 7.64 (d, 0.5H, J = 9.0 Hz, QnH-5), 7.18−7.04 (m, 6H, PhH + QnH-6), 6.59 (s_{br}, 0.5H, NH), 6.43 (d, 1H, J = 5.9 Hz, QnH-3), 6.25 (s_{br}, 0.5H, NH), 4.24 (d, 2H, J = 12.9 Hz, NCH_2), 4.18 (m, 1H, H-Cp), 4.12 (m, 1H, H-Cp), 4.01 (s, 5H, H-Cp′), 4.00 (m, 1H, H-Cp), 3.63 (t, 0.5H, J = 6.4 Hz, CH), 3.57 (t, 0.5H, J = 6.4 Hz, CH), 3.49 (d, 0.5H, J = 12.3 Hz, NCH_2), 3.37 (d, 0.5H, J = 12.3 Hz, NCH_2), 3.30 (d, 0.5H, J = 12.3 Hz, NCH_2), 3.22 (d, 0.5H, J = 12.3 Hz, NCH_2), 2.22 (m, 6H, CH_2 + H-Pip), 2.02 (m, 2H, CH_2), 1.39 (m, 4H, H-Pip), 1.28 (m, 2H, H-Pip). ^{13}C NMR (75 MHz, $CDCl_3$) δ (ppm): 152.1 (CH), 149.6 (C), 149.2 (C), 146.7 (C), 134.8 (C), 128.6 (CH), 128.5 (CH), 127.3 (CH), 127.0 (CH), 125.1 (CH), 123.5 (CH), 118.5 (C), 99.7 (CH), 85.9 (C), 84.3 (C), 70.0 (CH), 69.1 (CH), 66.5 (CH), 64.2 (CH), 61.7 (CH), 56.2 (CH_2), 54.5 (CH_2), 45.8 (CH_2), 42.0 (CH_2), 34.3 (CH_2), 25.9 (CH_2), 24.3 (CH_2). MS (ESI) m/z: 563 $MH^{+\ 37}Cl$, 609 $M^{+\bullet\ 37}Cl$, 608 $MH^{+\ 35}Cl$, 607 $M^{+\bullet\ 35}Cl$, 391 $(C_9H_5N^{37}ClNHCH_2C_{10}H_8FeCH_2)^+$, 389 $(C_9H_5N^{35}ClNHCH_2C_{10}H_8FeCH_2)^+$. Anal. $C_{35}H_{39}ClN_4Fe\cdot1.5H_2O$.

Time-Dependent Formation of Glutathione-Mannich Base Monoadducts. To a solution of 650 μL of H_2O and 250 μL of aqueous NH_4HCO_3 solution (25 μM), 50 μL of GSH (20 mM in H_2O) and 50 μL of the inhibitor (20 mM in DMSO) were added. The reaction mixture (pH 6.5−7) was incubated at room temperature. After different times, the solution was injected in HPLC to determine the Mannich base:monoSG-adduct versus time (min). The HPLC analysis was performed on a Hitachi Merck L-4000 equipped with a UV detector set at 254 nm. HPLC retention times were obtained using the following conditions: 100% eluent A (0.05% trifluoroacetic acid (TFA) in H_2O) for 5 min, a gradient up to 100% B (0.05% TFA in H_2O/CH_3CN (1:4) within 10 min, 100% B for 5 min, then again a gradient up to 100% A within 5 min at a flow rate of 1 mL/min.

Drugs. Ferroquine base (FQ), licensed as SR97193 today, was obtained from Prof. J. Brocard (France). Chloroquine diphosphate (CQ) was purchased from Sigma Aldrich, and quinine hydrochloride (QN) and monodesethylamodiaquine (MDAQ) were obtained from the World Health Organization (Geneva, Switzerland). FQ and synthetic compounds were resuspended and then diluted in RPMI-DMSO (99v/1v) to obtain final concentration ranging from 0.125 to 500 nM. CQ was resuspended in water in concentrations ranging between 5 and 3200 nM for CQ. QN and MDAQ were first dissolved in methanol and then diluted in water to obtain final concentrations ranging from 5 to 3200 nM and from 1.56 to 1000 nM, respectively.

Assay of β-Hematin Inhibition in Eppendorf Tubes. We determined the IC_{50} values for inhibition of β-hematin formation using Egan's test[35] with very slight modifications as described below. Drug solutions (44.6, 26.8, 13.4, 8.9, 6.7, 4.5, 2.2, 0.9 mM) were prepared by dissolving the drug in methanol/HCl 1:1. Hematin stock solution (1.68 mM) was prepared by dissolving bovine hemin (1.08 mg) in 0.1 M NaOH (986 μL). The solution was incubated at room temperature for 60 min. In a series of Eppendorf tubes, 4 μL of drug solution were dispensed and 12.9 M sodium acetate solution, pH 5.0, (11.7 μL) preincubated at 60 °C was added. Then the Eppendorf tubes were placed in an incubator at 60 °C. The β-hematin formation process was initiated by adding the hematin stock solution (20.2 μL) prepared above. The final hematin concentration was 1 mM, the final drug concentrations were 5, 3, 1.5, 1, 0.75, 0.5, 0.25, 0.1, and 0 mM, and the final solution pH was 4.5. The reaction mixtures were incubated at 60 °C for 60 min. After incubation, the reaction mixture was quenched at room temperature by adding 900 μL of 200 mM HEPES 5% (v/v) pyridine solution, pH 8.2, to adjust the final pH of the mixtures to a value between 7.2 and 7.5. Then, 1100 μL of 20 mM HEPES 5% (v/v) pyridine solution, pH 7.5, was added. The Eppendorf tubes were shaken, and the precipitate of β-hematin was scrapped from the walls of the Eppendorf tubes to ensure complete dissolution of hematin. The β-hematin was allowed to settle at room temperature for at least 15 min. The supernatant was carefully transferred to a cuvette without disturbing the precipitate, and absorption was measured at 405 nm.

In Vitro Antimalarial Activities. Parasite Cultures and Primary Screening Against NF54 and K1 *P. falciparum* Strains. CQ-Susceptible NF54 was cultivated in a variation of the medium previously described,[47] consisting of RPMI 1640 supplemented with 0.5% ALBUMAX II, 25 mM Hepes, 25 mM $NaHCO_3$ (pH 7.3), 0.36 mM hypoxanthine, and 100 μg/mL

neomycin. The chloroquine-, pyrimethamine-, and cycloguanil-resistant K1 strain (Thailand) of *P. falciparum* were acquired from MR4 (Malaria Research and Reference Reagent Resource Center, Manassas, VA). *P. falciparum* in vitro culture was carried out using standard protocols[47] with modifications. Briefly, parasites were maintained in tissue culture flasks in human A Rh+ erythrocytes at 5% hematocrit in RPMI 1640 supplemented with 25 mM HEPES, 24 mM $NaHCO_3$, 0.2% (w/v) glucose, 0.03% L-glutamine, 150 μM hypoxanthine, and 0.5% Albumax II (Invitrogen) in a 5% CO_2/air mixture at 37 °C, and the medium was changed daily. Asynchronous ring stage cultures were prepared at 1% parasitemia and 50 μL added per well, the top test drug final concentration being 30 μM. After 24 h incubation, 37 °C, 5% CO_2 5 μL (^{3}H)-hypoxanthine was added (0.2 μCi/well)[48] and plates were shaken for 1 min and then incubated for 48 h. The plates were freeze/thawed rapidly, harvested, and dried. (^{3}H)-hypoxanthine uptake was measured using a microbeta counter (Wallac 1450). IC_{50} values were calculated (Prism).

Parasite Cultures, Secondary Screening Against *P. falciparum* Strain Dd2. The IC_{50} was tested by standard in vitro antiproliferation assays.[48] Infected erythrocytes in ring stage (0.5% parasitemia, 2.5% hematocrit) in 96-well plates were exposed to the compounds for 48 h and then to radioactive hypoxanthine for 24 h. The amount of radioactivity in precipitable material served as an index of cell proliferation.

Parasite Cultures and Tertiary Screening Against Twelve Strains Expressing Varying Susceptibilities to Chloroquine and Quinine. Twelve parasite strains (well characterized laboratory strains or strains obtained from isolates after growth in culture for an extended period of time) from a wide panel of countries: Africa (3D7), Brazil (Bres), Cambodia (K2 and K14), Cameroon (FCM29), Djibouti (Voll), the Gambia (FCR3), Indochina (W2), Niger (L1), Senegal (8425), Sierra Leone (D6), and Uganda (PA)[49,50] were maintained in culture in RPMI 1640 (Invitrogen, Paisley, U.K.), supplemented with 10% human serum (Abcys SA, Paris, France) and buffered with 25 mM HEPES and 25 mM $NaHCO_3$. Parasites were grown in A-positive human blood under controlled atmospheric conditions that consists of 10% O_2, 5% CO_2, and 85% N_2 at 37 °C with a humidity of 95%. For in vitro isotopic microtests, 25 μL/well of antimalarial drug and 200 μL/well of the parasitized red blood cell suspension (final parasitemia, 0.5%; final hematocrit, 1.5%) were distributed into 96-well plates. Parasite growth was assessed by adding 1 μCi of tritiated hypoxanthine with a specific activity of 14.1 Ci/mmol (Perkin-Elmer, Courtaboeuf, France) to each well at time zero. The plates were then incubated for 48 h in a controlled atmospheric condition. Immediately after incubation, the plates were frozen and thawed to lyse erythrocytes. The contents of each well were collected on standard filter microplates (Unifilter GF/B, Perkin-Elmer) and washed using a cell harvester (Filter-Mate Cell Harvester, Perkin-Elmer). Filter microplates were dried, and 25 μL of scintillation cocktail (Microscint O, Perkin-Elmer) was placed in each well. Radioactivity incorporated by the parasites was measured with a scintillation counter (Top Count, Perkin-Elmer). The IC_{50}, defined as the drug concentration able to inhibit 50% of parasite growth, was assessed by identifying the drug concentration corresponding to 50% of the uptake of tritiated hypoxanthine by the parasite in the drug-free control wells. The IC_{50} value was determined by nonlinear regression analysis of log-based dose−response curves (Riasmart, Packard, Meriden, USA). The cutoff values, defined statistically (> 2 SD above the mean with or without correlation with clinical failures) for in vitro resistance or reduced susceptibility to CQ, QN, and MDAQ were 100, 800, and 60 nM, respectively.

In Vivo Antimalarial Activities. Compounds **2** and **3** were tested in the *P. berghei* ANKA mouse model by using the 4-day suppressive test, as indicated by Peters,[38] and using chloroquine as a positive control. Briefly, naive 18−20 g Swiss mice were infected intravenously with 2×10^6 parasitized red cells on day +0. For administration, compounds were freshly prepared in 10% DMSO in sterile phosphate-buffered saline the day of use. Two hours postinfection, mice received the first treatment by the intraperitoneal (ip) route. Mice were further treated on days +1−3. Blood films from tail blood were prepared on day +4, and parasitemia was determined by microscopic examination of Giemsa-stained blood films. Compounds **2** and **3** were tested at a daily dose of 30 mg/kg (**2**) or 50 mg/kg (**3**) by the ip route. Chloroquine treatment po at 10 mg/kg/day was included as a positive control and resulted in complete inhibition (data not shown). Intraperitoneal dosing of CQ have shown similar activity (98.9% inhibition at 10 mg/kg ip) in a number of tests but was not done specifically with this series of compounds. Mice were treated and levels of parasitemia determined as described.

Evaluation of the Cytotoxicity. Human MRC-5_{SV2} cells are cultured in Earls MEM + 5% FCSi. Assays are performed in 96-well microtiter plates, each well containing about 10^4 cell/well. After 3 days incubation, cell viability was assessed fluorimetrically after addition of resazurin and fluorescence was measured (λ_{ex} 550 nm, λ_{em} 590 nm). The results are expressed as % reduction in cell growth/viability compared to untreated control wells and CC_{50} is determined. Compounds are tested within the dose range of 0.25 μM. When the CC_{50} is lower than 4 μM, the compound is classified as highly toxic.

Proliferation Assays. Cells from the NCH89 glioblastoma cell line were cultured as described.[51] Proliferation assays were performed, as described,[52] using the BrdU Labeling and Detection Kit III (Roche Diagnostics, Germany). Cells (7×10^3 cells/well) were seeded in replicas in 96-well plates for 24 h. Then CQ, FQ, and drugs **1**−**5** were added in concentrations ranging from 0.1 to 100 μM to the wells, and 48 h later, BrdU was applied at a final concentration of 100 μM and measured according to the manufacturer's instructions.

DNA Binding Studies. Preparation of the Drug Solutions. Drug stock solutions (10 mM) were prepared by dissolving the drug in methanol or water according to its lipophilicity. TE buffer (10 mM Tris-HCl 0.1 mM EDTA, at pH 7.4) containing 5 mM NaCl was applied as buffer in the optical measurements.

Spectroscopic Characterization of the Compounds. UV absorption spectra between 220 and 380 nm were measured on a Cary 4E spectrophotometer and fluorescence spectra on an SLM-Aminco 8100 fluorimeter with excitation at 320 nm, detection between 340 and 500 nm. Fluorescence spectra were corrected for solvent signal and instrument response. Quartz cells of 1 cm optical path were applied filled with 2 mL of sample of 3 mM drug concentration. Spectra were registered in TE buffer containing 5 mM NaCl, in methanol and in toluene. The specific molar absorption coefficients were evaluated from the absorption spectra. The quantum yields in aqueous solution were determined relative to that of CQ by dividing the integrated emission spectra by the absorption at the common excitation wavelength and expressed as % of the quantum yield of CQ. In the case of the poorly emitting ferrocenic compounds, the Raman scattering was taken into correction.

Evaluation of Drug Binding with DNA. The spectral changes upon addition of DNA to the drugs were measured by absorption and fluorescence. Quartz cells of optical path length 3 mm were used with 100−150 μL samples. The binding experiments were accomplished by titrating a 1 or 10 μM drug solution with a linear pUC18 DNA solution (50% AT) measuring the absorption or fluorescence spectra at room temperature. The final concentrations of DNA in the cuvette were varying between 0.1 and 50 μM base pairs.

Optical Melting Measurements. Thermal denaturation curves of the DNA were recorded by absorbance at 260 nm on a Cary 4E spectrophotometer (Varian, Mulgrave, Australia) equipped with a Peltier thermoregulator and an automatic

cuvette changer. The samples contained 1 μM drug solution and DNA of 15 μM base pair concentration, with initial absorbance of 0.2 at 260 nm in quartz cells of 1 cm path length in TE buffer with 5 mM NaCl. The heating rate was 0.5 °C/min in the temperature range 30−97 °C, and the absorbance data were collected at every 0.5 °C. Data were treated using the program KaleidaGraph. The curves were normalized to the absorbance at room temperature and smoothed in five-point intervals. Derivative melting curves were calculated from the smoothed data and once more smoothed in five-point intervals. The maxima of the derivative melting curves were read as corresponding melting temperatures (T_m^{max}). To correct for differences in peak asymmetry, two further temperatures were calculated to characterize the melting: the middle of the peak at its half height ($T_m^{1/2}$) and the middle of the integrated surface below the derivative melting peak (T_m^{int}). Two types of DNA were used for this study: linear pUC18 DNA (containing 50% AT) and synthetic polydAdT (100% AT)

Acknowledgment. We are grateful to B. Jannack and M. Brückner, who contributed by excellent technical assistance to the chemical preparation of starting materials in bulk, to HPLC measurements and in performing the hematin polymerization assays, respectively. Dr. G. Furrer is acknowledged for recording ^{1}H, ^{13}C NMR spectra (Organisch-Chemisches Institut, Heidelberg University). Dr. A. Page is acknowledged for recording the mass spectra (Centre Commun de Mesures de l'Université des Sciences et Technologies de Lille). The authors thank R. Amalvict, E. Baret, and J. Mosnier for technical support (Institut de Recherche Biomédicale des Armées—Antenne de Marseille). Our work is supported by the CNRS-DFG program of the Centre National de la Recherche Scientifique (E.D.C.) and by the Deutsche Forschungsgemeinschaft (SFB 544 "Control of Tropical Infectious Diseases", B14 project (E.D.C.)). N.W. is grateful for a fellowship from the SFB544-DFG program. A BDI fellowship from CNRS and Region Nord-Pas-de-Calais to N.C. is gratefully acknowledged. We are grateful to the PROCOPE program that supported this French−German collaboration. This investigation received financial support from the UNICEF/UNDP/World Bank/WHO Special Programme for Research and Training in Tropical Diseases (TDR).

Supporting Information Available: Glutathionylation rates of saturated Mannich bases **6** and **7** as Michael acceptors, absorption spectra of CQ, FQ, and their related analogues **1**−**5** measured in aqueous solution, IC_{50} and IC_{90} values of 4-aminoquinolines **1**−**5** against various *P. falciparum* strains, calculated and measured pK_a and log *D* values of some representatives in the organic series, specific molar absorption coefficients and relative quantum yields of CQ, FQ, and 4-aminoquinolines **1**−**5** measured in aqueous solution, specific molar absorption coefficients of CQ, FQ, and 4-aminoquinolines **1**−**5** measured in organic solvents, melting temperatures values of 50% and 100% AT-rich DNA evidencing their interaction with CQ, FQ, and 4-aminoquinolines **1**−**5**, and elemental analyses of new compounds **2**, **3**, and **5**. This material is available free of charge via the Internet at http://pubs.acs.org.

References

(1) Neftel, K. A.; Woodtly, W.; Schmid, M.; Frick, P. G.; Fehr, J. Amodiaquine induced agranulocytosis and liver damage. *Br. Med. J.* **1986**, *292*, 721–723.
(2) Egan, T. J.; Mavuso, W. W.; Ncokazi, K. K. The mechanism of beta-hematin formation in acetate solution. Parallels between hemozoin formation and biomineralization processes. *Biochemistry* **2001**, *40*, 204–213.
(3) Zarchin, S; Krugliak, M; Ginsburg, H. Digestion of the host erythrocyte by malaria parasites is the primary target for quinoline-containing antimalarials. *Biochem. Pharmacol.* **1986**, *35*, 2435–2442.
(4) Egan, T. J.; Chen, J. Y.-J.; de Villiers, K. A.; Mabotha, T. E.; Naidoo, K. J.; Ncokazia, K. K.; Langford, S. J.; McNaughton, D.; Pandiancherri, S.; Wood, B. R. Haemozoin (β-haematin) biomineralization occurs by self-assembly near the lipid/water interface. *FEBS Lett.* **2006**, *580*, 5105–5110.
(5) Egan, T. J. Recent advances in understanding the mechanism of hemozoin (malaria pigment) formation. *J. Inorg. Biochem.* **2008**, *102*, 1288–1299.
(6) Slater, A. F. G. Malaria Pigment. *Exp. Parasitol.* **1992**, *74*, 362–365.
(7) Sanchez, C. P.; Stein, W.; Lanzer, M. Trans stimulation provides evidence for a drug efflux carrier as the mechanism of chloroquine resistance in *Plasmodium falciparum*. *Biochemistry* **2003**, *42*, 9383–9394.
(8) Sanchez, C. P.; McLean, J. E.; Stein, W.; Lanzer, M. Evidence for a substrate specific and inhibitable drug efflux system in chloroquine resistant *Plasmodium falciparum* strains. *Biochemistry* **2004**, *43*, 16365–16373.
(9) Sanchez, C. P.; McLean, J. E.; Rohrbach, P.; Fidock, D. A.; Stein, W. D.; Lanzer, M. Evidence for a pfcrt-associated chloroquine efflux system in the human malarial parasite *Plasmodium falciparum*. *Biochemistry* **2005**, *44*, 9862–9870.
(10) Sanchez, C. P.; Rohrbach, P.; McLean, J. E.; Fidock, D. A.; Stein, W. D.; Lanzer, M. Differences in trans-stimulated chloroquine efflux kinetics are linked to PfCRT in *Plasmodium falciparum*. *Mol. Microbiol.* **2007**, *64*, 407–420.
(11) Gilberger, T.-W.; Schirmer, R. H.; Walter, R. D.; Müller, S. Deletion of the parasite-specific insertions and mutation of the catalytic triad in glutathione reductase from chloroquine-sensitive *Plasmodium falciparum* 3D7. *Mol. Biochem. Parasitol.* **2000**, *107*, 169–179.
(12) Meierjohann, S.; Walter, R. D.; Müller, S. Regulation of intracellular glutathione levels in erythrocytes infected with chloroquine-sensitive and chloroquine-resistant. *Plasmodium falciparum*. *Biochem J.* **2002**, *368*, 761–768.
(13) Chavain, N.; Davioud-Charvet, E.; Trivelli, X.; Mbeki, L.; Rottmann, M.; Brun, R.; Biot, C. Antimalarial antimalarial activities of ferroquine conjugates with either glutathione reductase inhibitors or glutathione depletors via a hydrolyzable amide linker. *Bioorg. Med. Chem.* **2009**, *17*, 8048–8059.
(14) Iley, J.; Constantino, L. Oxidation of tertiary benzamides by 5,10,15,20-tetraphenyl porphyrinatoiron^{III} chloride−*tert*-butylhydroperoxide. *Org. Biomol. Chem.* **2004**, *2*, 1894–1900.
(15) Bazin, M. J.; Shi, H.; Delaney, J.; Kline, B.; Zhu, Z.; Kuhn, C.; Berlioz, F.; Farley, K. A.; Fate, G.; Lam, W.; Walker, G. S.; Yu, L.; Pollastri, M. P. Efficient use of the iron ortho-nitrophenylporphyrin chloride to mimic biological oxidations of dimethylaminoantipyrine. *Chem. Biol. Drug Des.* **2007**, *70*, 354–359.
(16) Bernadou, J.; Meunier, B. Biomimetic chemical catalysts in the oxidative activation of drugs. *Adv. Synth. Catal.* **2004**, *346*, 171–184.
(17) Meunier, B. Hybrid molecules with a dual mode of action: dream or reality? *Acc. Chem. Res.* **2008**, *41*, 69–77.
(18) Meunier, B.; de Visser, S. P.; Shaik, S. Mechanism of oxidation reactions catalyzed by cytochrome P_{450} enzymes. *Chem. Rev.* **2004**, *104*, 3947–3980.
(19) Irvin, J. L.; Irvin, E. M.; Parker, F. S. The interaction of antimalarials with nucleic acids. *Science* **1949**, *110*, 426–428.
(20) Meshnick, S. R. Chloroquine as intercalator: a hypothesis revived. *Parasitol. Today* **1990**, *6*, 77–79.
(21) Ginsburg, H.; Nissani, E.; Krugliak, M.; Williamson, D. H. Selective toxicity to malaria parasites by non-intercalating DNA-binding ligands. *Mol. Biochem. Parasitol.* **1993**, *58*, 7–15.
(22) Parker, F. S.; Irvin, J. L. The interaction of chloroquine with nucleic acids and nucleoproteins. *J. Biol. Chem.* **1952**, *199*, 897–909.
(23) Stollar, D.; Levine, L. Antibodies to denaturated deoxyribonucleic acid in lupus erythematosus serum. V. Mechanism of DNA-anti-DNA inhibition by chloroquine. *Arch. Biochem. Biophys.* **1963**, *101*, 335–341.
(24) Kurnick, N. B.; Radcliffe, I. E. Reaction between DNA and quinacrine and other antimalarials. *J. Lab. Clin. Med.* . **1962**, *60*, 669–688.
(25) Bolton, P. H.; Mirau, P. A.; Shafer, R. H.; James, T. L. Interaction of the antimalarial drug fluoroquine with DNA, tRNA, and poly(A): ^{19}F-NMR chemical-shift and relaxation, optical absorption, and fluorescence studies. *Biopolymers* **1981**, *20*, 435–449.
(26) Allison, J.-L.; O'Brien, R. L.; Hahn, F. E. DNA: reaction with chloroquine. *Science* **1965**, *149*, 1111–1113.

(27) Cohen, S. N.; Yielding, K. L. Spectrophotometric studies of the interaction of chloroquine with deoxyribonucleic acid. *J. Biol. Chem.* **1965**, *240*, 3123–3131.
(28) Cheng, J.; Zeidan, R.; Mishra, S.; Liu, A.; Pun, S. H.; Kulkarni, R. P.; Jensen, G. S.; Bellocq, N. C.; Davis, M. E. Structure−function correlation of chloroquine and analogues as transgene expression enhancers in nonviral gene delivery. *J. Med. Chem.* **2006**, *49*, 6522–6531.
(29) Pollack, Y.; Katzen, A. L.; Spira, D. T.; Golenser, J. The genome of *Plasmodium falciparum* I: DNA base composition. *Nucleic Acids Res.* **1982**, *10* (2), 539–546.
(30) Kwakye-Berko, F.; Meshnick, S. R. Sequence preference of chloroquine binding to DNA and prevention of Z-DNA formation. *Mol. Biochem. Parasitol.* **1990**, *39*, 275–278.
(31) Kwakye-Berko, F.; Meshnick, S. R. Binding of chloroquine to DNA. *Mol. Biochem. Parasitol.* **1989**, *35*, 51–56.
(32) Woynarowski, J. M.; Krugliak, M.; Ginsburg, H. Pharmacogenomic analyses of targeting the AT-rich malaria parasite genome with AT-specific alkylating drugs. *Mol. Biochem. Parasitol.* **2007**, *154*, 70–81.
(33) Baxter, E. W.; Reitz, A. B. Reductive aminations of carbonyl compounds with borohydride and borane reducing agents. *Organic Reactions* **2004**, *59*, 1–57.
(34) Glorian, G.; Maciejewski, L.; Brocard, J.; Agbossou, F. Enantioselective synthesis of (*R*)- and (*S*)-1-ferrocenylalkylamines. Reduction of enantiopure ferrocenylimines obtained from valinol and phenylglycinol. *Tetrahedron: Asymmetry* **1997**, *8*, 355–358.
(35) Ncokazi, K. K.; Egan, T. E. A colorimetric high-throughput β-hematin inhibition screening assay for use in the search for antimalarial compounds. *Anal. Biochem.* **2005**, *338*, 306–319.
(36) Chavain, N.; Vezin, H.; Dive, D.; Touati, N.; Paul, J. F.; Buisine, E.; Biot, C. Investigation of the redox behavior of ferroquine, a new antimalarial. *Mol. Pharm.* **2008**, *5*, 710–716.
(37) Buisine, E.; de Villiers, K.; Egan, T. J.; Biot, C. Solvent-Induced Effects: Self-Association of Positively Charged π Systems. *J. Am. Chem. Soc.* **2006**, *128*, 12122–12128.
(38) Peters, W.; Robinson, B. L. *Handbook of Animal Models of Infection*; Academic Press, London: 1999; pp 756−771.
(39) Rajapakse, C. S.; Martínez, A.; Naoulou, B.; Jarzecki, A. A.; Suárez, L.; Deregnaucourt, C.; Sinou, V.; Schrével, J.; Musi, E.; Ambrosini, G.; Schwartz, G. K.; Sánchez-Delgado, R. A. Synthesis, characterization, and in vitro antimalarial and antitumor activity of new ruthenium(II) complexes of chloroquine. *Inorg. Chem.* **2009**, *48*, 1122–1131.
(40) Remy, J. S.; Sirlin, C.; Vierling, P.; Behr, J. P. Gene transfer with a series of lipophilic DNA-binding molecules. *Bioconjugate Chem.* **1994**, *5*, 647–654.
(41) Viola, G; Salvador, A; Cecconet, L; Basso, G; Vedaldi, D; Dall'Acqua, F; Aloisi, G. G.; Amelia, M; Barbafina, A; Latterini, L; Elisei, F. Photophysical properties and photobiological behavior of amodiaquine, primaquine and chloroquine. *Photochem. Photobiol.* **2007**, *83*, 1415–1427.
(42) Aravind, L.; Iyer, L. M.; Wellems, T. E.; Miller, L. H. Plasmodium biology: genomic gleanings. *Cell* **2003**, *115*, 771–785.
(43) Davioud-Charvet, E.; McLeish, M. J.; Veine, D. M.; Giegel, D.; Arscott, L. D.; Andricopulo, A. D.; Becker, K.; Muller, S.; Schirmer, R. H.; Williams, C. H., Jr.; Kenyon, G. L. Mechanism-based inactivation of thioredoxin reductase from *Plasmodium falciparum* by Mannich bases. Implication for cytotoxicity. *Biochemistry* **2003**, *42*, 13319–13330.
(44) Friebolin, W.; Jannack, B.; Wenzel, N.; Furrer, J.; Oeser, T.; Sanchez, C. P.; Lanzer, M.; Yardley, V.; Becker, K.; Davioud-Charvet, E. Antimalarial Dual Drugs Based on Potent Inhibitors of Glutathione Reductase from *Plasmodium falciparum*. *J. Med. Chem.* **2008**, *51*, 1260–1277.
(45) Perrine, D. M.; Sabanayagam, N. R.; Reynolds, K. J. Synthesis of NMP, a fluoxetine (Prozac) precursor, in the introductory organic laboratory. *J. Chem. Educ.* **1998**, *75*, 1266.
(46) Tsuji, T.; Mizuma, T.; Toyoshima, S. Chemotherapeutic drugs against viruses. XXVII. Synthesis and antiviral activity of 1-(*p*-alkylphenyl)-3-dimethylamino-1-propanol. *Chem. Pharm. Bull.* **1960**, *8*, 763–767.
(47) Trager, W.; Jensen, J. B. Human malaria parasites in continuous culture. *Science* **1976**, *193*, 673–675.
(48) Desjardins, R. E.; Canfield, C. J.; Haynes, J. D.; Chulay, J. D. Quantitative assessment of antimalarial activity in vitro by a semiautomated microdilution technique. *Antimicrob. Agents Chemother.* **1979**, *16*, 710–718.
(49) Henry, M.; Briolant, S.; Zettor, A.; Pelleau, S.; Baragatti, M.; Baret, E.; Mosnier, J.; Amalvict, R.; Fusai, T.; Rogier, C.; Pradines, B. *Plasmodium falciparum* Na^+/H^+ exchanger 1 transporter is involved in reduced susceptibility to quinine. *Antimicrob. Agents Chemother.* **2009**, *53*, 1926–1930.
(50) Parquet, V.; Briolant, S.; Torrentino-Madamet, M.; Henry, M.; Almeras, L.; Amalvict, R.; Baret, E.; Fusai, T.; Rogier, C.; Pradines, B. Atorvastatin is a promising partner for antimalarial drugs in treatment of *Plasmodium falciparum* malaria. *Antimicrob. Agents Chemother.* **2009**, *53*, 2248–2252.
(51) Herold-Mende, C.; Steiner, H. H.; Andl, T.; Riede, D.; Buttler, A.; Reisser, C.; Fusenig, N. E.; Mueller, M. M. Expression and functional significance of vascular endothelial growth factor receptors in human tumor cells. *Lab Invest.* **1999**, *79*, 1573–1582.
(52) Biot, C.; Taramelli, D.; Forfar-Bares, I.; Maciejewski, L. A.; Boyce, M.; Nowogrocki, G.; Brocard, J. S.; Basilico, N.; Olliaro, P.; Egan, T. J. Insights into the mechanism of action of ferroquine. Relationship between physicochemical properties and antiplasmodial activity. *Mol. Pharmaceutics* **2005**, *2*, 185–193.